N^5-Methylasparagine and Energy-Transfer Efficiency in C-Phycocyanin†

Beth Ann Thomas,‡,§ Lloyd P. McMahon,‖ and Alan V. Klotz*,‡,⊥

Departments of Biochemistry and Chemistry, Louisiana State University, Baton Rouge, Louisiana 70803

Received June 28, 1994; Revised Manuscript Received December 27, 1994⊗

ABSTRACT: A posttranslationally methylated asparagine residue, N^5-methylasparagine, is found at the β-72 site in many phycobiliproteins. Two mutations (Asp and Gln) in the β-72 position of *Agmenellum quadruplicatum* C-phycocyanin were investigated to clarify the role of the wild-type N^5-methylasparagine near the β-84 "fluorescing" bilin tetrapyrrole chromophore. Chemical analysis for amide modification revealed that the β-72Q protein was partially methylated with a stoichiometry of 0.27, suggesting that either the asparagine methyltransferase is nonspecific or a glutamine methyltransferase exists. Urea denaturation studies could detect no difference in protein stability for any of the C-phycocyanin species. Steady-state spectroscopic measurements demonstrate that Asp and Gln substitution for the C-phycocyanin β-72 NMA affects both the ground to excited state transition and the excited-state characteristics of the β-84 chromophore, while the rate of radiative energy transfer is unaffected. Energy-transfer efficiency within phycobilisomes (represented by steady-state fluorescence quantum yields) was also negatively impacted by the β-72 substitutions. Time-resolved fluorescence emission spectroscopic studies with C-phycocyanin reveal three distinguishable fluorescence lifetimes. The longest fluorescence lifetime is diminished 7−10% by the Asp and Gln mutations in comparison to a control sample where β-72 is NMA. Molecular dynamics calculations implicate a change in the bilin tetrapyrrole chromophore ring geometry as a likely source of the altered photophysics induced by the mutations. We conclude that N^5-methylasparagine plays a special role in establishing the environment surrounding the β-84 chromophore which minimizes the rates of nonradiative energy losses that would otherwise defeat the high quantum yield for energy transfer within the phycobilisomes.

Phycobiliproteins are unique pigment proteins found in cyanobacteria, cryptomonads, and red algae that function as light-harvesting antennae. These proteins form macromolecular aggregates known as phycobilisomes that electrostatically interact with the stromal side of the thylakoid membrane in the vicinity of photosystem II. They function to absorb excitation energy in the range of 450−650 nm with energy transfer to the protein−chlorophyll complex of PS II (Glazer, 1989; Bryant, 1986) in a process which occurs with >95% quantum efficiency (Searle *et al.*, 1978). Many studies exploring structure−function relationships in phycobiliproteins have been accomplished to address energy-transfer rates through the phycobilisome (Glazer *et al.*, 1985a,b; Searle *et al.*, 1978) and spectroscopic studies of the bilin chromophores (Lagarias *et al.*, 1988; Mimuro *et al.*, 1986). In addition to the well-described thioether-linked bilin tetrapyrroles, Klotz *et al.* (1986) reported an unusual posttranslational methylation of asparagine, N^5-methylasparagine (γ-*N*-methylasparagine). N^5-Methylasparagine has been found in many phycobiliproteins isolated from prokaryotic cyanobacteria, from eukaryotic red algae, and more recently from the highly divergent eukaryotic cryptomonads (Klotz & Glazer, 1987; Rümbeli *et al.*, 1987; Wilbanks *et al.*, 1989). The X-ray crystal structures of several phycobiliproteins have been solved at high resolution (Duerring *et al.*, 1988, 1991; Schirmer *et al.*, 1986, 1987), making this an attractive system for detailed studies. The conserved methylated asparagine is present at position 72 in the β subunit at 1 Molar equiv., while no α subunits contain the modification. Sequence information indicates that, in the exceptional β subunits which lack NMA,[1] the conserved asparagine residue at position β-72 has been replaced with either glycine or proline, a two-base change in the genetic code (Klotz & Glazer, 1987).

An analogous amide methylation of glutamine, δ-*N*-methylglutamine, is present in *Escherichia coli* ribosomal protein L3 in stoichiometric quantities at a single site (Lhoest & Colson, 1977). The mutant *prm*B2, which lacks the methylase activity responsible for glutamine methylation, displays a cold-sensitive phenotype and a diminished rate of ribosome assembly (Lhoest & Colson, 1981). However, these ribosomes are fully active once assembled, suggesting that glutamine methylation affects only the assembly process. Prior to the study of NMA, glutamine methylation represented the sole instance in which *N*-methylation of a protein

† This research was supported in part by a grant from the U.S. Department of Agriculture, NRIGCP 91-37306-6868.

* Author to whom correspondence should be addressed.

‡ Department of Biochemistry.

§ Current address: Department of Entomology, University of California, Davis, CA 95616.

‖ Department of Chemistry.

⊥ Current address: Novo Nordisk Biotech, Inc., 1445 Drew Avenue, Davis, CA 95616.

⊗ Abstract published in *Advance ACS Abstracts,* February 15, 1995.

[1] Abbreviations: APC, allophycocyanin; AU, absorbance units; β-72D, Asn→Asp substitution at the C-phycocyanin β-72 position; β-72Q, Asn→Gln substitution at the C-phycocyanin β-72 position; C-PC, C-phycocyanin; *cpc*BA/BA, control strain where genomic phycocyanin genes are inactivated by transposon insertion and the wild-type C-phycocyanin genes are plasmid encoded; DAS, decay-associated emission spectra; NMA, N^5-methylasparagine (γ-*N*-methylasparagine); NMG, N^6-methylglutamine (δ-*N*-methylglutamine); PS II, photosystem II; SDS−PAGE, sodium dodecyl sulfate-polyacrylamide gel electrophoresis; 7002, *Agmenellum quadruplicatum* PCC 7002 wild-type cells.

0006-2960/95/0434-3758$09.00/0

amino acid could be correlated with an identifiable function.

The focus of this report is to elucidate the role of asparagine posttranslational methylation in the phycobiliprotein C-phycocyanin. Previous experiments involving two independently isolated asparagine methyltransferase mutants from *Synechococcus* PCC 7942 have shown that asparagine methylation is associated with enhanced quantum yields of oxygen evolution (~14%) and increased photosynthetic efficiency (Swanson & Glazer, 1990; Thomas *et al.*, 1993). This suggests that the β-72 methylation is associated with increased energy-transfer efficiency from phycobilisome components to the terminal energy acceptors in photosystem II. The presence of NMA is also associated with a selective growth advantage under low-light conditions to cells which contain the modification (B. A. Thomas and A. V. Klotz, unpublished observations). However, the interpretation of these latter data derived from chemically generated mutants is complicated by the possibility of additional unrecognized genetic lesions in the proteins. To avoid this confounding aspect, we turned to techniques of site-specific mutagenesis.

The goal of our current studies is to substantiate the hypothesis that NMA uniquely interacts with the β-84 tetrapyrrole chromophore thereby optimizing transfer efficiency within phycobiliprotein aggregates. To this end we investigated two site-specific mutants of *Agmenellum quadruplicatum* C-PC which possess either Asp or Gln in the place of NMA. The β-72D mutant was constructed in order to test the hypothesis that placement of a negative charge in the proximity of the fluorescing chromophore would cause electrostatic repulsion with the propionic acid side chain which could alter chromophore geometry or, alternatively, increase the likelihood of chromophore deprotonation. The β-72Q mutant was constructed to test the possibility of altered chromophore orientation due to the substitution of an *N*-methyl group with a methylene group. This mutant was also constructed to test for the possibility of glutamine methylation which would inform on questions of methyltransferase specificity.

A wealth of structure−function studies aimed at elucidating the fundamental aspects of energy transfer within the phycobilisome have established that the 300−1000 bilin chromophores in a phycobilisome unit are organized to achieve rapid directional energy transfer via nonradiative Förster-type mechanisms [e.g., Gillbro *et al.* (1985) and Glazer *et al.* (1985 a,b)]. The intramolecular transfer step (within a phycocyanin $[\alpha\beta]_6$ disk unit) occurs in less than 8 ps, which is within the dead time of many instruments, while the distinguishable transfer steps occur between phycobilisome disk units with half-times of ~20 ps. The C-phycocyanin X-ray crystal structure indicates that each of the three bilin chromophores is found in a slightly different protein environment, thus differentiating the chromophore classes (Schirmer *et al.*, 1986, 1987). The β-72 NMA proximal to the β-84 chromophore is one of the unique features of the environment surrounding this "fluorescing" chromophore which is responsible for directional interdisk energy transfer within the phycobilisome structure.

Sauer and colleagues (Sauer *et al.*, 1987; Debreczeny *et al.*, 1993) have refined the original sensitizing/fluorescing chromophore concept of Teale and Dale (1970) and presented an "mfs" model for the evolution of fluorescence within the C-PC monomer. The essential elements of this model are that the excited states for all three chromophores are in equilibrium with each other. In the C-PC monomer the α-84 chromophore does not efficiently transfer excitation energy to the other chromophores. Energy transfer from β-155 to β-84 is rapid (τ = ~50 ps), while the α-84 and β-84 are major contributors to the medium (τ = ~600 ps)- and slow (τ = 1500 ps)-fluorescing components, respectively.

The conceptual framework in which our fluorescence experiments were performed and interpreted is as follows: The inverse of the measured lifetime, τ^{-1}, is equal to the sum of the radiative and nonradiative rates, $\tau^{-1} = k_r + k_{nr}$. We demonstrate in this report that the relative extinction coefficients are identical for control and mutant C-PC; this establishes that the radiative rate, k_r, remains unchanged if the Franck−Condon principle holds for this system. We additionally report that β-72 replacement confers decreased fluorescence quantum yields for both isolated C-PC and phycobilisomes. Given that k_r is unaffected, an increase in Σk_{nr} must occur in the mutants to effect an overall decrease in quantum yield. Therefore, the Asp and Gln mutations decrease energy-transfer efficiency by depopulating the excited state of the chromophore.

EXPERIMENTAL PROCEDURES

Mutant Construction. Genetic engineering at the β-72 sequence position was accomplished by J. Zhou, Pennsylvania State University (Zhou, 1992). Mutations in the C-phycocyanin β subunit were constructed on the 1.69-kb *Bgl*II−*Xho*I fragment of plasmid pAQPR1 (de Lorimier *et al.*, 1984) and inserted into the *Bam*HI−*Sal*I site of plasmid pUC9. The appropriate modified genes were introduced into the biphasic shuttle vector plasmid pAQE19 by cloning into the *Hin*dIII−*Eco*RI site. PCC 7002 strain PR6230 was transformed with the shuttle vector, followed by selection for antibiotic resistance. Strain PR6230 contains a transposon (K_m^r) insertion into the genomic *Bgl*II−*Xho*I site which replaces the *cpc*A, *cpc*B, and a portion of the *cpc*C genes; this effectively yields a *cpc*ΔBAC phenotype. *cpc*C encodes the 33-kDa linker polypeptide; absence of this linker causes the phycobilisomes to have shortened rods. Therefore, a control strain is used in which PR6230 is transformed with wild-type *cpc*BA genes (Swanson *et al.*, 1992). Protein expression in a *Synechococcus* PCC 7002 background is essential to ensure proper chromophorylation and phycobilisome assembly.

Strains and Culture Conditions. Synechococcus PCC 7002 (wild-type *Agmenellum quadruplicatum*) was grown at 32−37 °C in medium A supplemented with 1 mg/mL $NaNO_3$ (Stevens *et al.*, 1973). Media for genetically engineered strains was supplemented with 50 μg/mL ampicillin and 200 μg/mL kanamycin. The cultures were constantly stirred and infused with 4% CO_2 and were maintained at a temperature of 32−34 °C for 10-L carboys and 35−36 °C for 1-L Fernbachs. Light was provided by cool-white fluorescent bulbs at an intensity of 90−100 μmol of photons/m^2/s. Growth rates of wild-type, control, and mutant strains were determined by analysis of chlorophyll concentration as a function of time (Williams, 1988). The doubling times for 7002 wild type, *cpc*BA/BA, β-72D, and β-72Q were 15, 33, 25 and 29 h, respectively.

C-Phycocyanin Isolation. Cells of 7002 wild type, control, and mutants were grown in 10-L carboys, harvested approximately 2 weeks post-inoculation, stored at 4 °C, and

broken (Glazer & Bryant, 1975), and the C-PC was purified (Glazer & Fang, 1973). C-PC purity was examined spectroscopically and by SDS−PAGE to assure >95% purity. Purified C-PC was subjected to gel filtration chromatography on a 1.5 × 60 cm BioGel P-60 column in 20 mM $NaPO_4$, pH 7.0, using sample concentrations of 0.03, 0.09, and 0.26 mg/mL to determine the aggregation state. The column was calibrated using bovine serum albumin (66 kDa), chicken ovalbumin (43 kDa), horse heart myoglobin (16.5 kDa), and horse heart cytochrome *c* (12.4 kDa).

Phycobilisome Isolation. Phycobilisomes were prepared by a procedure similar to that of Bryant *et al.* (1979). All buffers contained 0.75 M $NaKPO_4$ (pH 7.0), 1 mM β-mercaptoethanol, and 1 mM NaN_3. Wild-type and mutant phycobilisomes were concurrently prepared at room temperature. Phycobilisomes were recovered free of contaminating chlorophyll from 0.6 M sucrose for the engineered mutants and from the 0.8 M layer for wild type. Phycobilisome preparations were assessed spectroscopically and by analysis on 10−15% linear gradient SDS−PAGE for purity. Sucrose was removed from the phycobilisome samples by repeated ultrafiltration washing using a PM-10 membrane (Diaflo Corp.) with 0.75 M $NaKPO_4$ (pH 7.0).

Isoelectric Focusing. Isoelectric focusing was accomplished by using the Pharmacia PhastGel system with the buffer system of Yamanaka *et al.* (1982). The pH gradient was calibrated through the use of isoelectric focusing standards (pH 3.6−9.3; Sigma Chemical Co.).

Methylation Analysis. The control strain (*cpc*BA/BA), β-72D, and β-72Q were radiolabeled with [*methyl*-^{3}H]-methionine (200 μCi/μmol), and subsequently C-PC was purified, acid hydrolyzed, and subjected to amino acid analysis as described previously (Thomas *et al.*, 1993).

Absorbance Spectroscopy. Absorbance spectra were acquired every 1 nm using a Uvikon 810 spectrophotometer (Kontron Instruments, Switzerland) with a bandwidth of 2 nm. Relative extinction coefficients were determined as in Lundell and Glazer (1983). Briefly, C-PC absorption spectra were acquired in 20 mM $NaPO_4$, pH 7.0, containing 1 mM NaN_3, and the absorption spectra were reacquired after samples had been diluted with 3 vol of 8 M guanidine hydrochloride−5% (v/v) formic acid to yield a final 6 M guanidine hydrochloride solution. The bilin maximal absorbance in 6 M guanidine hydrochloride was normalized to the maximal absorbance of C-PC under native conditions to determine the relative extinction coefficient.

Protein Stability Measurements. Purified C-PC from wild type, control, and site-directed mutants was exhaustively dialyzed in 20 mM $NaPO_4$, pH 7.0, 1 mM β-mercaptoethanol, and 1 mM NaN_3 prior to denaturation experiments. All unfolding studies were accomplished in 20 mM NaAc (pH 5.5), containing 5 mM β-mercaptoethanol, and 1 mM NaN_3.

Ultrapure grade urea (>99.9% purity) was purchased from Amresco, and a 10 M stock was used for all denaturation experiments. The various urea concentrations were prepared gravimetrically by weighing out the appropriate amount of urea from the 10 M stock. The correct mass of urea was calculated from the density of a 10 M urea solution [recalculated from Kawahara and Tanford (1966)]. The appropriate amount of acetate buffer was then added to the flask, and the contents were thoroughly mixed with a Pasteur pipette. Finally, C-PC was added to the urea solution at a concentration of 0.1−0.2 mg/mL; the final volume was adjusted to 1 mL. Urea-containing samples were prepared in the region of 0−8 M in 0.5 M increments. All samples were allowed to equilibrate at room temperature for at least 30 min prior to spectroscopic measurement. The kinetics of refolding was examined by monitoring the change in absorbance intensity at the visible wavelength maximum for the bilin chromophore. Unfolding was initiated in 8 M urea; protein samples were allowed to incubate for at least 30 min (15 min is required to completely unfold wild-type C-PC under these experimental conditions). Refolding was initiated by dilution into acetate buffer to achieve a final urea concentration of 1−3 M. Refolding was measured by acquiring a wavelength scan in the region of 800−300 nm every 5 min.

Wavelength scans for absorption during unfolding and refolding were obtained in the region of 800−250 nm in either 0.5- or 1-nm increments. C-PC was prepared for fluorescence measurement by diluting the prepared urea-containing samples with acetate buffer to obtain a final concentration of 0.05 or 0.1 AU at the excitation wavelength of 580 nm. Steady-state fluorescence spectra were acquired by scanning emission from 600 to 700 nm using a 1−3-s time constant.

CD Spectroscopy. Circular dichroism measurements were accomplished on an AVIV 62DS spectrometer in which the wavelength range of 215−230 nm was recorded in 0.5-nm increments employing a 0.7-nm bandwidth and a 1.0-s time constant. Sample temperature was regulated at 25 °C by a circulating water bath. The instrument was calibrated using a freshly prepared solution of (+)-10-camphorsulfonic acid at a concentration of 0.92 mg/mL as measured by the absorbance at 285 nm. The spectra were collected by signal averaging three to six individual scans; the data were baseline-corrected using the instrument software. For these stability experiments the absorbance of C-PC approached 1.0 AU in a 0.1 cm pathlength cuvette.

Steady-State Fluorescence Spectroscopy. Fluorescence spectra were acquired with an SLM 8000 spectrofluorimeter interfaced to a MacIIcx using software written with the LabVIEW program (Stryjewski, 1991). Magic angle polarizers were set to 55° for excitation and 0° for emission; this architecture circumvents the common diffraction grating attribute that horizontal light is not transmitted at certain wavelengths. Monochromator slits and lamp voltage were adjusted so that the intensity of the emitted light was favorable for single-photon counting detection (≥40 000 counts). For steady-state emission the spectral bandwidths were set at 4 and 2 nm for excitation and emission, respectively. All measurements were made with the emission monochromator 90° to excitation. The absorbance at the excitation wavelength of 580 nm was 0.05 AU for purified C-PC and 0.2 AU for phycobilisome samples. Steady-state emission spectra were collected by scanning the emission monochromator from 600 to 800 nm at a rate of 5 s/nm. Emission spectra were corrected for buffer absorbance and for wavelength-dependent instrument response by using correction factors determined with a standard Optronics lamp.

Time-Resolved Fluorescence. Fluorescence lifetime measurements were accomplished utilizing time-correlated single-photon counting on a Photochemical Research Associates instrument with a picosecond dye laser excitation source. The instrument has been described in detail by McMahon *et al.* (1992). For these experiments the output beam from

the dye laser (rhodamine 6G dye) was passed through a Newport 935 attenuator to adjust the intensity. The fundamental light from the dye laser was used because frequency doubling was not required for this excitation wavelength. The fluorescence emission was detected by a cooled Hamamatsu R955 multichannel plate photomultiplier, amplified by a PRA 1763 fast preamplifier, and discriminated by an Ortec 583 constant fraction discriminator. The R955 photomultiplier was operated at 3150 V across the first dynode. The width of the instrument response was 50−80 ps FWHM. An excitation wavelength of 580 nm was selected with a three-plate birefringent filter. The exciting light was vertically polarized; the emission polarizer was oriented at 55°. The emission wavelength was selected with an Instruments SA H-10 monochromator at 8 nm bandpass. The excitation rate was 760 kHz; emission rates were <10 kHz. The cell holder temperature was maintained with a circulating bath at 25 °C. All samples were matched at an absorbance of 0.1 AU at 580 nm (the excitation wavelength) in 20 mM $NaPO_4$, pH 7.0; this concentration corresponds to ~0.015 mg/mL. Debreczeny *et al.* (1993) have calculated that 580-nm light will preferentially excite the β-155 chromophore in the C-PC monomer; however, approximately 50% of the relative absorption will be contributed by the sum of the α-84 and β-84 chromophores. Emission was detected from 620 to 670 nm in 10-nm increments.

The fluorescence decays of the sample and the instrument response function were acquired contemporaneously in 1024 channels of 7.33 ps/channel to approximately 2.5×10^4 counts in the peak. The instrument was controlled by a Macintosh IIcx computer operating data acquisition software developed using the National Instruments control software LabVIEW (Stryjewski, 1991). A solution of glycogen in water was used to collect the instrument response function.

The decay curves were deconvolved and analyzed as sums of exponential decays by using the "Globals Unlimited" fluorescence package (Beecham *et al.*, 1989). The goodness-of-fit to a physical model was determined by the magnitude of the reduced χ^2, the shape of the autocorrelation function, and analysis of the weighted residual errors. Analysis of fluorescence decay data involved identification of the most appropriate model that described the data. The validity of the determined lifetimes was tested by iteratively fixing one or more of the linked lifetimes while allowing the remaining lifetimes to be determined by the program. A well-defined lifetime was considered to be one which was continually determined in the analysis when other lifetimes were fixed to selected values; the determined lifetimes were robust. The data were additionally analyzed by unlinked analysis of the individual decay curves so as to approximate the variance associated with a particular lifetime. In this manner, the lifetimes for wild type and mutants were amenable to statistical analysis. Individual decay curves as a function of emission wavelength were fit to a double/triple-exponential decay. The resulting lifetimes and preexponential factors are reported as an average ± standard deviation for either eight or nine experiments. The differences in lifetimes between the control and mutants were tested for statistical significance at the 95% confidence interval by applying a two-sided test of variance and Satterthwaite's theorem (Satterthwaite, 1946). This statistical exercise was accomplished using the Minitab software program.

The decay-associated emission spectra were calculated by using the equation

$$I_i(\lambda) = I(\lambda)\alpha_i(\lambda)\tau_i / \sum \alpha_i(\lambda)\tau_i$$

where $I_i(\lambda)$ is the corrected steady-state emission intensity, α_i is the amplitude of component i at the specified wavelength, and τ_i is the lifetime at wavelength i (Tilstra *et al.*, 1990).

Molecular Mechanics/Dynamics. The X-ray crystal structure coordinates of the C-PC trimer from *Mastigocladus laminosus* were kindly provided by Dr. Marcus Duerring (Schirmer *et al.*, 1987). All mechanics and dynamics calculations were accomplished in the program CHARMM on the β subunit of C-PC (Brooks *et al.*, 1983). The nonstandard monomer units such as NMA and phycocyanobilin were manually built according to known atom parameters (Schirmer *et al.*, 1986).

The β subunit was routinely minimized to a final root mean square deviation of approximately 0.1 kcal/Å prior to any manipulation to remove unfavorable steric conflicts. Truncation of nonbonded interactions was accomplished by the use of a switched potential function with a range of 6.5−7.5 Å and a cutoff of 8 Å. A dielectric $\epsilon = 4r$ (r = distance in Å) was used for all calculations. The molecular dynamics trajectory encompassed a total of 70 ps *in vacuo* dynamics by using the Verlet algorithm and included heating, equilibration, and cooling phases. The heating/preequilibration phase consisted of 10 ps in which the temperature was increased from 0 to 300 K in 30° increments every 100 steps. The equilibration phase consisted of 10 ps at 300 K in which the velocities were scaled to a final temperature every 500 steps. The production phase then followed for 50 ps in which there was total energy conservation. The production phase was quenched to 0 K at 10-ps intervals by decreasing the temperature by 30° every 100 steps. The end point conformers were extensively energy minimized to a final RMS deviation of 0.02−0.05 kcal/Å. Analysis of the C-PC β subunit dynamics was based on examination of these minimized endpoint conformers and time correlation series of the production phase in the dynamics trajectory.

RESULTS

Characterization of β-72 Mutations. The B72D and B72Q site-specific mutants have similar phenotypes in that they both appear more yellowish in color than wild type in culture. The engineered mutants grow at a slower rate than wild-type PCC 7002 under identical illumination conditions. Whole-cell absorption spectra of the mutants show a substantial reduction in the amount of phycobiliprotein relative to chlorophyll with a 41% decrease for the genetically engineered control and mutant strains. It is possible that the lower observed ratio could be due to a change in the molar extinction coefficient for the mutant β subunits caused by a change in chromophore environment. This hypothesis was tested, and it was found that the relative extinction coefficients for the two engineered mutants are indistinguishable from that for *cpc*BA/BA (Table 1). Indeed, deletion of the *cpc*C gene in the engineered constructs causes the phycobilisomes to have shortened rods as a result of fewer phycocyanin-containing disk elements.

Confirmation of β-72 replacement with either Asp or Gln was addressed at the protein level by two different meth-

Table 1: Relative Extinction Coefficients of Site-Directed Mutants[a]

cell type	A_{max} (native)	A_{max} (bilin)	rel extinction coeff.
*cpc*BA/BA (β-72 = NMA)	1.60	0.140 ± 0.008 (5)	2.86
β-72D	1.69	0.147 ± 0.003 (4)	2.87
β-72Q	1.66	0.143 ± 0.003 (3)	2.90

[a] The relative extinction coefficient was determined n independent times (numbers in parentheses) by dividing the native absorbance by the bilin absorbance after taking into account the 1:4 dilution of the denatured samples (see Experimental Procedures).

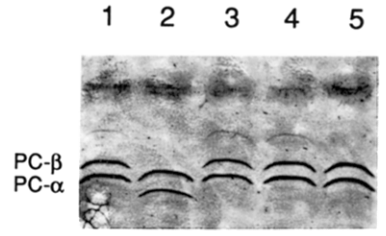

FIGURE 1: Isoelectric focusing of purified C-phycocyanin in the presence of 8 M urea: *cpc*BA/BA (lane 1), β-72D (lane 2), β-72Q (lane 3), *cpc*BA/BA (lane 4), and 7002 wild type (lane 5); 1.5 μg was loaded per lane, and the protein was detected by Coomassie R-250 staining.

ods: isoelectric focusing and radiolabel analysis. The change from NMA to Asp is predicted to decrease the net charge of the protein. Figure 1 shows the results of isoelectric focusing in the presence of urea. The β subunit of β-72D C-PC demonstrates a decrease in p*I* by 0.1 unit as compared to the control, while the corresponding β-72Q substitution results in no p*I* change (as expected). The p*I* was also calculated from the known amino acid sequence by using the "Isoelectric" algorithm (University of Wisconsin Genetics Computer Group software). This calculation approximates the experimental data, although the p*I*s are uniformly decreased by ~0.3 unit for both the α and β subunits. Introduction of Asp causes a calculated decrease of 0.3 charge unit relative to the control for the β subunit. The β-72Q mutant shows no change in β subunit p*I* by either determination method, as expected for a conservative substitution.

An additional method by which Asp or Gln introduction can be indirectly examined at the protein level is by analysis of radiolabeled methyl incorporation into C-PC. Substitution of β-72 NMA with Asp should result in a loss of the stoichiometric methylamine peak present in amino acid analysis of C-PC acid hydrolysates. The presence of methylamine in a putative Asp mutant would imply that the mutant has reverted to wild type. Second, the presence of radiolabeled methylamine in the β-72Q construct would suggest that the Gln amide nitrogen is methylated. The primary rationale for preparation of tritiated β-72Q was to examine possible methylation by an unspecified methyltransferase activity. This experiment does not distinguish between Gln and NMA at the β-72 site; i.e., reversion of the Gln mutant to methylated wild type is not testable by this method.

The control strain (*cpc*BA/BA) was radiolabeled in parallel with β-72D and β-72Q. There are nine methionines and one NMA per [$\alpha\beta$] monomer in *Agmenellum quadruplicatum* C-PC (de Lorimier *et al.*, 1984); two of the methionines are present at the NH_2-termini of the α and β subunits (Gardner

Table 2: ^{3}H-Radiolabel Analysis of Engineered C-Phycocyanin[a]

strain	[methylamine]/C-PC [$\alpha\beta$]
*cpc*BA/BA	1.11 ± 0.10 (2)
β-72D	<0.05[b]
β-72Q	0.27 ± 0.06 (4)

[a] [methylamine]/C-PC [$\alpha\beta$] was quantitated by determining the radiochemical ratio of methylamine to methionine in acid hydrolysates of purified phycobiliproteins. [b] Below the experimental limit of detection.

et al., 1980). We assumed that all methionines have incorporated a labeled methyl group. Thus, the theoretical methylamine/C-PC [$\alpha\beta$] for *cpc*BA/BA should be 1.00; the experimentally observed value for two replicate experiments is 1.11 ± 0.10. There is no detectable methylamine in the β-72D C-PC hydrolysis products. Table 2 shows the results of radiolabel analysis of β-72Q in which the average methylamine/C-PC [$\alpha\beta$] is 0.27, suggesting that ~27% of the available glutamine sites are methylated. An alternative explanation for methylation at this site could be the reversion of β-72Q to wild-type; however, our spectroscopic data below argue against this possibility.

Characterization of Wild-Type and Mutant C-Phycocyanins. Our previous studies have demonstrated that asparagine methylation improves photosynthetic capabilities of cells containing the modification under conditions in which the phycobilisomes are preferentially illuminated (Thomas *et al.*, 1993). Therefore, it was concluded that asparagine methylation improves the light-harvesting efficiency of phycobilisomes. It was our goal to spectroscopically characterize the β-72D and β-72Q mutants in both isolated phycobiliproteins and their corresponding phycobilisomes in order to substantiate the hypothesis of improved phycobilisome energy transfer in the presence of NMA.

The effects of β-72 substitution on the spectroscopic characteristics of purified C-PC were first examined. Gel filtration chromatography for the control and mutant proteins under the dilute conditions (0.03 mg/mL) of the spectroscopic experiments and 3-fold higher concentrations resulted in elution with an apparent molecular mass of 38 000−40 000 Da. This establishes that the purified C-PC was in a monomeric aggregation state under dilute conditions. Experiments at much higher protein concentrations (0.26 mg/mL) revealed measurable aggregation by the control C-PC (migration corresponding to 62 000 Da), while the β-72D and β-72Q mutants displayed apparent molecular masses of 45 000 and 56 000 Da, respectively. Therefore, aggregation can only be detected at protein concentrations which are more than 3-fold greater than the conditions of our fluorescence experiments.

The effects of NMA substitution with Asp or Gln are revealed in the difference spectra as shown in Figure 2. The presence of NMA at β-72 appears to increase the intensity of a ground to excited state transition on the red side of the C-PC absorption envelope. Therefore, the energy difference between the ground and excited states of the β-84 fluorescing chromophore is perturbed by NMA replacement. These data are congruent with those of Swanson and Glazer (1990) in which the absorption spectra of two methyltransferase mutants (β-72 = Asn) demonstrate a small blue shift in the absorption spectra as compared to wild-type (β-72 = NMA). The substitution of NMA with Asp or Gln causes a

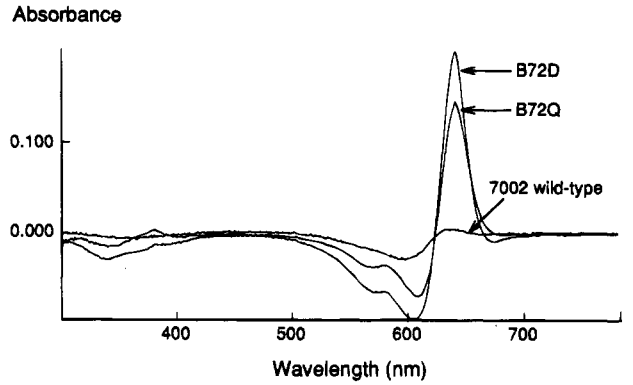

FIGURE 2: Difference absorption spectra of purified C-phycocyanin. All spectra recorded at protein concentrations of approximately 0.12 mg/mL were normalized by computer at λ_{max}, and the differences were obtained by subtraction of the spectrum of interest from that of *cpc*BA/BA.

Table 3: Spectroscopic Characterization of Phycobiliproteins and Phycobilisomes[a]

strain	A_{max} (nm)	F_{max} (nm)	ϕ_f[b]
7002 (wild-type)			
phycobilisomes	630	659	1.05
C-phycocyanin	624	644	1.02
cpc BA/BA (control)			
phycobilisomes	635	671	1.0
C-phycocyanin	624	644	1.0
β-72D			
phycobilisomes	631	666	0.86
C-phycocyanin	617	642	0.78
β-72Q			
phycobilisomes	632	667	0.96
C-phycocyanin	620	644	0.92

[a] Absorbance spectra were acquired from 800 to 300 nm in 0.75 M $NaKPO_4$, pH 7.0, for phycobilisomes (0.1−0.25 mg/mL) and in 20 mM $NaPO_4$, pH 7.0, for C-phycocyanin (0.05−0.1 mg/mL). Fluorescence emission spectra were acquired from 600 to 800 nm with excitation at 580 nm at protein concentrations of approximately 0.03 mg/mL for phycobilisomes and 0.008 mg/mL for C-PC. [b] Fluorescence quantum yields are normalized to the control strain (*cpc*BA/BA).

reproducible blue shift of 7 or 3 nm, respectively, in the λ_{max} as summarized in Table 3. NMA at β-72 obviously alters the absorption characteristics of the β-84 chromophore. The fluorescence spectra of the β-72D and β-72Q mutants demonstrate that a negligible blue shift and a decrease in emission quantum yield of 22 and 8%, respectively, occur upon NMA replacement (Figure 3). These data are consistent with less efficient energy transfer within the C-PC monomer.

Wild-Type and Mutant Phycobilisome Characterization. The effects of NMA substitution on the spectroscopic properties of higher aggregates such as phycobilisomes were examined. Phycobilisomes were isolated from 0.2−1.0 M sucrose gradients in which the wild-type aggregates banded in 0.8 M sucrose while the control and mutants banded in 0.6 M sucrose. Banding of wild-type phycobilisomes in 0.8 M sucrose is a direct consequence of the presence of the 33-kDa linker polypeptide encoded by the *cpc*C gene. The absence of the 33-kDa linker as illustrated in SDS−PAGE of purified phycobilisomes from the control and mutant strains provides further confirmation of successful mutation (data not shown).

The effect of substitutions at the β-72 site on the spectroscopic properties of phycobilisomes was examined by both absorbance and steady-state fluorescence emission. The phycobilisomes that contained Asp and Gln at the C-PC β-72 site exhibited small blue shifts in λ_{max} of 4 and 2 nm, respectively, relative to the control that are consistent with the shifts observed for C-PC from the corresponding strains (Table 3). The fluorescence emission maxima for the control and mutant strains are in the range of 666−671 nm and are attributed to fluorescence emanating from the terminal emitters of the phycobilisome core. A mutation in the C-PC rod components is not expected to cause a significant change in the phycobilisome maximal fluorescence wavelength. The replacement of NMA in C-PC does result in diminished fluorescence emission quantum yields in phycobilisomes, however, indicating that the rod components absorb and transfer excitation energy less efficiently to the terminal acceptors in the core (Table 3). The Asp mutant demonstrates a fluorescence quantum yield that is decreased 14% from the control, while β-72Q displays a modest decrease of 6%; this is in agreement with our previous oxygen-evolution studies of the methyltransferase mutants. The β-72D and β-72Q mutants displayed a prominent blue band in the 0.2 M sucrose region whose intensity varied among preparations. This blue band consists of detached phycobilisome rods judging by the blue-shifted maximal fluorescence at ~650 nm. This fluorescence wavelength coincides with that of phycobilisomes which were incubated in low phosphate to intentionally cause phycobilisome dissociation involving loss of rod-to-core energy transfer caused by rod detachment from the core. One might infer from these results that NMA improves the stability of rod linker polypeptide to allophycocyanin core interactions that maintain a functional phycobilisome. The alternative possibility for dissociation would be the more extensive fragmentation of the rods into various aggregation states of C-PC. This is not the case because the λ_{max} values of C-PC monomers for the Asp and Gln mutants are blue-shifted at 642 and 644 nm, respectively, and thus phycobilisome samples would be shifted by up to 20 nm if the samples contained C-PC fragments.

Effects of β-72 Substitution on Protein Stability. The effects of site-specific β-72 NMA substitution on C-PC stability were examined as a result of the apparent effect on phycobilisome stability. The unfolding of C-PC as induced by urea was monitored by using several different spectroscopic techniques so that independent measures of conformational stability could be obtained. Absorbance was used to monitor changes in the bilin chromophore environment by evaluation of both the visible absorbance peak at ~620 nm and the near-ultraviolet peak at ~350 nm. The visible maximal absorbance is a sensitive parameter for following protein unfolding evidenced by the change in absorbance upon denaturation. Circular dichroism was additionally used as an independent measure of protein structure. The native CD spectrum displays a minimum at 222 nm that is characteristic of α-helical structure. The denatured protein shows a very weak signal that is 5-fold lower in intensity and is devoid of helical nature.

Conformational stability of proteins was examined by analyzing urea denaturation profiles. Calculation of the free energy for unfolding assumes that the protein of interest undergoes a two-state reversible unfolding transition with no intermediates along the folding pathway. The buffer system 20 mM NaAc, pH 5.5 yielded favorable conditions

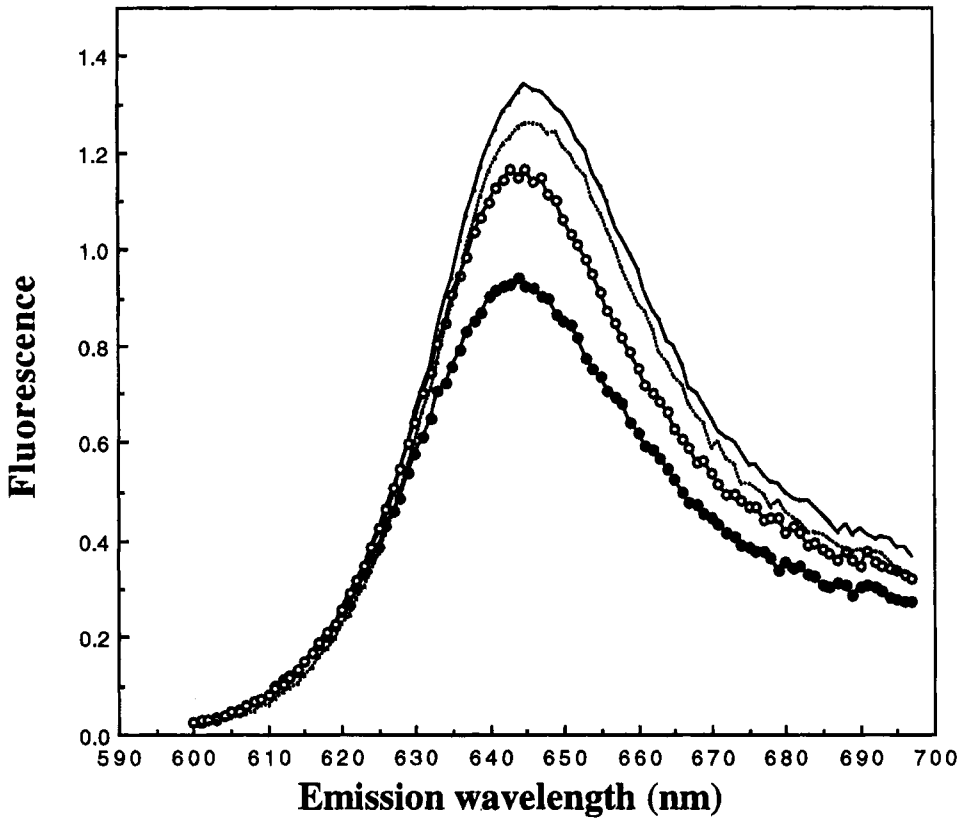

FIGURE 3: Corrected fluorescence emission spectra of purified C-phycocyanin. 7002 wild type is represented by a solid line, *cpc*BA/BA is a dotted line, β-72D is shown as filled circles, and β-72Q is shown as open circles. All samples were matched at an absorbance of 0.05 AU at 580 nm. Spectra were acquired by scanning emission from 600 to 700 nm with excitation at 580 nm. Spectra were corrected for wavelength-dependent instrument response.

Table 4: Parameters of Urea Denaturation of C-Phycocyanin[a]

protein	$\Delta G(H_2O)$ (kcal/mol)	m^b (kcal/mol/M)	$(urea)_{1/2}$ (M)	$\Delta(\Delta G)^c$ (kcal/mol)
PCC 7002 (β-72 = NMA)	7.91 ± 1.9 (2)[d]	1.72 ± 0.46	4.65 ± 0.15	+0.16
cpc BA/BA (β-72 = NMA)	10.2 ± 1.3 (2)[d]	2.23 ± 0.34	4.58 ± 0.08	
cpc β-72D	10.9 ± 1.7 (3)[d]	2.48 ± 0.43	4.42 ± 0.09	−0.36
cpc β-72Q	9.87 ± 2.2 (2)[d]	2.20 ± 0.47	4.49 ± 0.02	−0.20

[a] The midpoint of the cooperative unfolding transition is described as $[urea]_{1/2} = \Delta G(H_2O)/m$. [b] m describes the dependence of the free energy on urea concentration. [c] $\Delta(\Delta G) = \Delta([urea]_{1/2}) \times m$ (control). [d] Number of independent experimental measurements. For each independent experiment the CD and visible absorption spectrum data were combined to calculate ΔG.

for reversible refolding of C-PC as judged by absorbance spectroscopy. The protein was successfully renatured in 1 M urea to yield an absorbance spectrum that was essentially superimposable with the comparable native C-PC in 1 M urea (data not shown). All strains were shown to reversibly fold under these experimental conditions. It is intriguing that the most favorable refolding conditions were identified at a pH that is so near to the p*I* (~pH 5.6); however, there was no evidence of precipitation for 7002 C-PC. Furthermore, gel filtration analyses of C-PC from wild type, control, and mutants under these buffer conditions yields dimers/trimers.

The conformational stability of C-PC was evaluated by analysis of urea-induced unfolding profiles. Table 4 lists the calculated parameters from the results of these unfolding studies for wild-type, control, and mutant C-PC. The extrapolated $\Delta G(H_2O)$ was calculated by using the combined CD and absorbance data; all values are within experimental error of each other with the exception of 7002 wild type. There was >10% uncertainty in this calculation which might mask small differences in stability. Deviations of up to 30% in determination of $\Delta G(H_2O)$ by the linear extrapolation method have been reported (Pace & Vanderburg, 1979).

Time-Resolved Fluorescence Studies of Site-Directed Mutants. Fluorescence lifetimes were determined for C-PC in order to further dissect the impact of these mutations on the chromophore biophysics. The β-72 substitutions are expected to cause alterations in fluorescence lifetimes because both the lifetimes and the quantum yields depend on competition between radiative emission by fluorescence and processes that deactivate the excited state by nonradiative pathways. Analysis of our decay data first involved identification of the most appropriate physical model. A triple-exponential function was found to best describe the data in almost every case. Figure 4 shows the fit of a single β-72D data set to both a double and a triple exponential; it is obvious on the basis of the pattern of the autocorrelation function that the data are best fitted to a triple-exponential decay. The Globals Unlimited analysis program was used in two different manners to deconvolve the fluorescence decays. Each decay component for the data set was deconvolved both individually and linked to other decays for the same protein

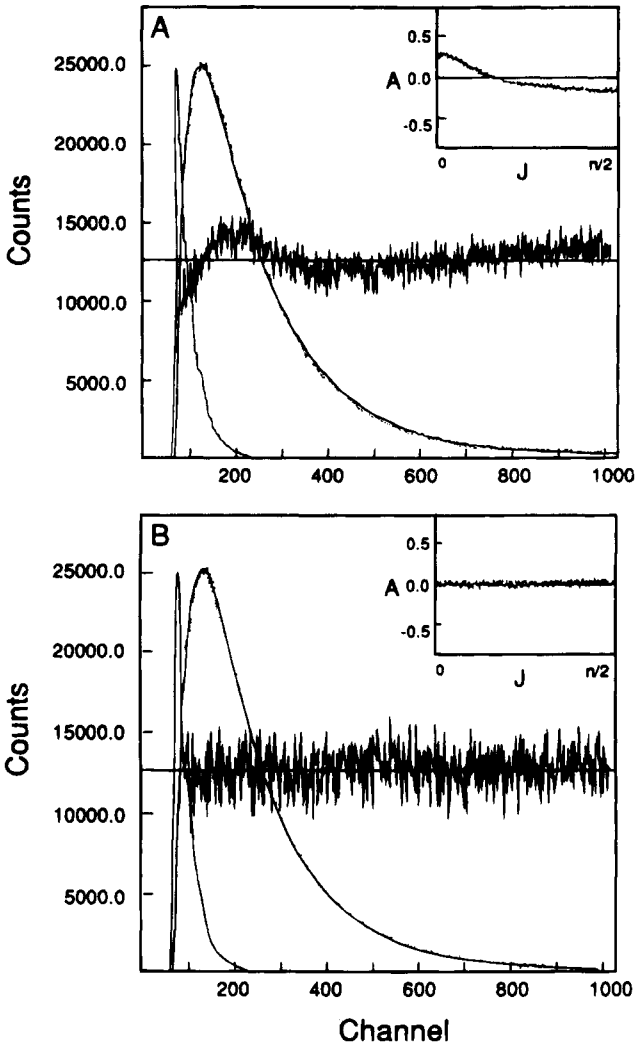

FIGURE 4: Fluorescence decays of β-72D C-PC. Excitation and emission wavelengths were 580 and 650 nm, respectively. The leftmost curve in each panel is the lamp reference curve. Data points are the sample decay, and the continuous line through the points represents the best fit to the following: (A) A double-exponential function where $\tau_1 = 1.22$ ns, $\tau_2 = 0.40$ ns, $\alpha_1 = 4.56$, $\alpha_2 = 1.49$, $Q = -0.34$, and $\chi^2 = 2.71$. (B) A triple-exponential function where $\tau_1 = 1.28$ ns, $\tau_2 = 0.62$ ns, $\tau_3 = 0.09$ ns, $\alpha_1 = 3.76$, $\alpha_2 = 2.26$, $\alpha_3 = -0.70$, $Q = -1.03$, and $\chi^2 = 1.05$. The autocorrelation function of the residual errors (inset) and the weighted residual errors are also shown. Time resolution was 7.33 ps/channel.

sample. The individual data files at each emission wavelength were fit to a triple-exponential decay function to obtain average lifetimes ± standard deviations. These data are shown in Table 5. The χ^2 values for the C-PC lifetimes were near unity, indicating a good statistical fit to the model, although τ_3 was not well determined in most data sets, which is reflected by its large relative standard deviations.

Differences in lifetimes caused by β-72 replacement were evaluated by using the average of the unlinked discrete data. This method of analysis allows an evaluation of differences between control and mutant lifetimes after consideration of experimental error. Variance calculations were conducted to establish the statistical significance of the differences between control and mutant lifetimes. Indications of significant differences between control and mutants at the 95% confidence interval are listed in Table 5. Introduction of Asp and Gln into the β-72 site causes a 10 and 7% decrease for C-PC, respectively, in τ_1 and an 11 and 12% decrease, respectively, in τ_2. The differences in τ_3 were not considered to be significant due to the difficulty in parameter determination by either the linked global or the discrete analysis. These data are consistent with those obtained by steady-state methods and indicate that substitution of NMA increases nonradiative decay processes that depopulate the β-84 chromophore excited state and lead to reduced energy-transfer efficiency.

Table 5: Analysis of Monomeric C-Phycocyanin Fluorescence Lifetimes[a]

strain	τ_1 (ns)	τ_2 (ns)	τ_3 (ns)	χ^2
		Unlinked Analysis		
7002	1.40 ± 0.02	0.75 ± 0.05	0.08 ± 0.01	1.03 ± 0.09 (8)
*cpc*BA/BA	1.43 ± 0.06	0.78 ± 0.11	0.05 ± 0.04	1.20 ± 0.27 (8)
β-72D	1.29[b] ± 0.01	0.62[b] ± 0.02	0.07 ± 0.04	1.03 ± 0.03 (9)
β-72Q	1.33[b] ± 0.02	0.66[b] ± 0.02	0.07 ± 0.03	1.06 ± 0.05 (9)
		Linked Global Analysis		
7002	1.39	0.76	0.07	1.06
*cpc*BA/BA	1.39	0.75	0.07	1.07
β-72D	1.28	0.62	0.09	1.04
β-72Q	1.34	0.67	0.08	1.07

[a] Fluorescence lifetimes were determined by both an unlinked and a linked global analysis. Unlinked lifetime analysis values of the decay curves are reported as an average ± standard deviation for *n* datasets (numbers in parentheses). These data were analyzed by simultaneous global analysis in which the lifetimes were constrained to be the same for all emission wavelengths. [b] Significantly different from *cpc*BA/BA at the 95% confidence interval ($P < 0.05$).

The fluorescence decay data were also examined by simultaneous global analysis of the fluorescence decay curves in which the lifetimes were constrained to be the same for all emission wavelengths. This calculation method is advantageous because it solves for desired parameters over a larger data set, thus resulting in improved sensitivity and accurate parameter determination for the model. Table 5 presents the results of a global analysis for the emission-dependent data. Global analysis yields lifetimes and goodness-of-fit parameters that are comparable to those derived from the unlinked data sets for C-PC. Consequently, a global analysis of lifetimes across the emission band adequately describes the emission characteristics. The introduction of either Asp or Gln into the β-72 site decreases the observed lifetimes, which is consistent with an increase in nonradiative rate processes in these mutants.

The resolution of time-resolved components as a function of emission wavelength in these lifetime experiments has been accomplished by fitting to an impulse decay function to yield a decay-associated spectrum (DAS). The relevance of the observed lifetime differences upon NMA replacement was considered in the context of the calculated DAS. An examination of the DAS (Figure 5) for C-PC reveals that the relative contributions of the lifetime components as a function of emission wavelength are similar to each other. While no assignments for observed differences in τ_3 were made, this lifetime displays an intriguing negative rise term in the control strain, which is attributed to indirect excitation via energy transfer. This rise term is absent in the β-72 mutants, suggesting that the chromophore(s) contributing to τ_3 in the mutants are indirectly excited to a lesser extent by energy transfer. Consequently, energy transfer between sensitizing and fluorescing chromophores could be perturbed.

Molecular Mechanics/Dynamics of C-PC. It is our goal to corroborate the experimental data with theoretical calcula-

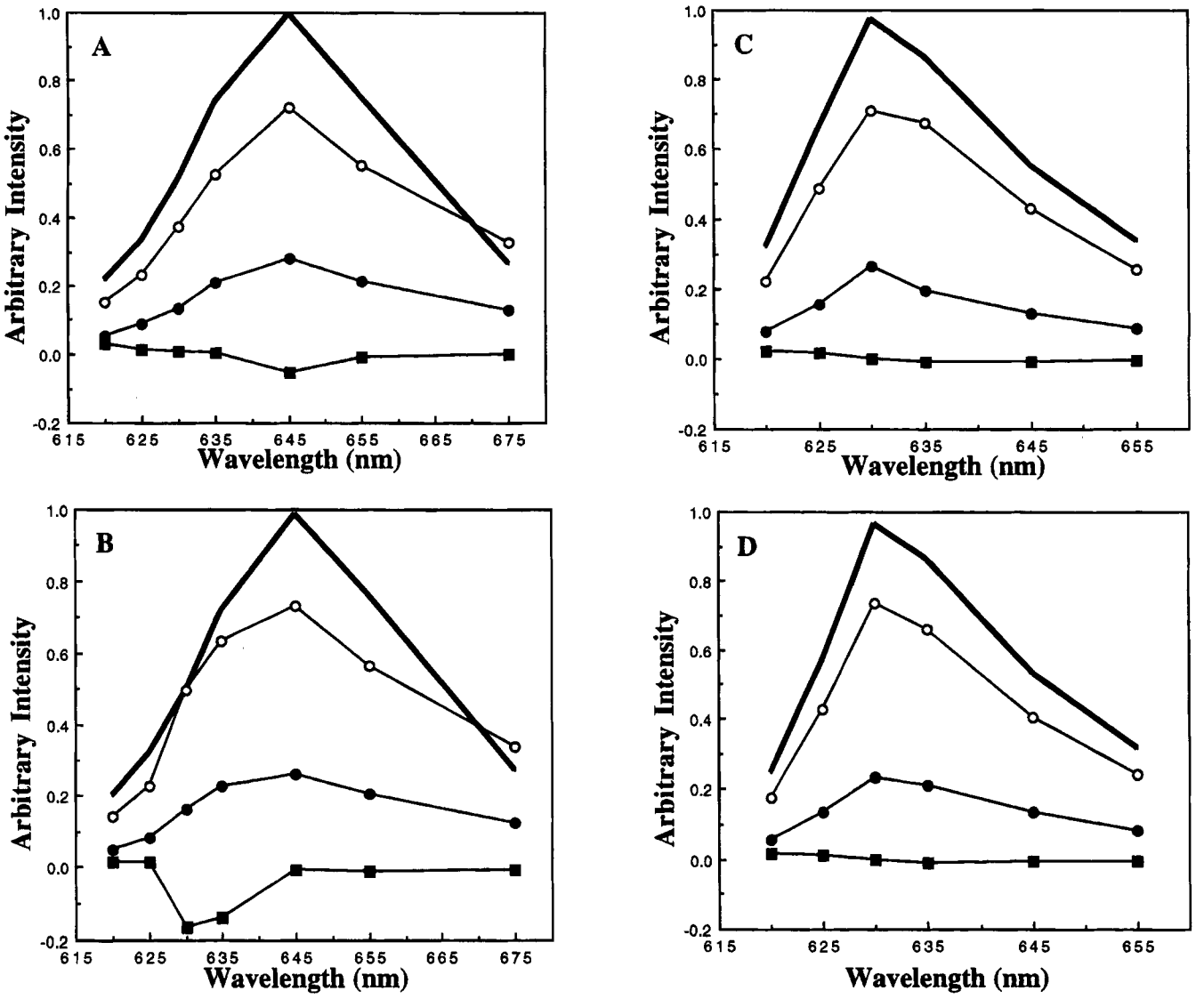

FIGURE 5: Decay-associated spectra (DAS) of C-phycocyanin: (A) 7002 wild type, (B) *cpc*BA/BA, (C) β-72D, and (D) β-72Q. In each panel, the steady-state emission spectrum is shown as a thickened line, τ_1 is represented by open circles, τ_2 is represented by closed circles, and τ_3 is represented by squares.

tions using the crystal structure of C-PC from *Mastigocladus laminosus* (Schirmer *et al.*, 1987). Molecular dynamics calculations were performed on C-PC with various replacements at the β-72 NMA site in order to evaluate perturbations in the local protein environment and the proximal β-84 chromophore. Changes in chromophore structure upon NMA substitution would expand the evidence that NMA improves energy-transfer efficiency and provide another indication that asparagine methylation serves a physiologically relevant biological function.

The effects of β-72 mutation were evaluated with reference to several parameters: main-chain and side-chain dihedral angles, local hydrogen-bonding networks, and β-84 chromophore geometry. Table 6 shows the main-chain and side-chain dihedral angles for each of the mutations as derived from the minimized end-point conformers. Removal of the NMA methyl group to yield Asn results in no significant changes in main-chain or side-chain dihedrals. However, replacement of NMA with an Asp creates deviations of 39° and 95°, respectively, for ψ and χ_1. The dihedral angles for Gln, δ-*N*-methylglutamine, and Ser substitutions at β-72 are similar to those with Asp. It is intriguing that even though

Table 6: Main- and Side-Chain Dihedral Angles at β-72[a]

β-72 amino acid	ψ	ϕ	χ_1
NMA	6.2 ± 4.3	−84.4 ± 3.9	−83.5 ± 17
Asn	−6.6 ± 2.6	−93.9 ± 12	−92.9 ± 36
Asp	−42.3 ± 18	−90.1 ± 8.6	−165 ± 10
Gln	−67.0 ± 5.7	−107 ± 28	−159 ± 18
Ser	−83.0 ± 2.8	−55.8 ± 2.3	−146 ± 60
NMG	−57.1 ± 2.6	−83.2 ± 2.0	−158 ± 2.5

[a] Dihedral angles were determined as an average ± standard deviation for the 3−4 endpoint minimized conformers.

Gln is nearly isosteric with NMA, its dihedral angles show large deviations. The determining factor for these angles is likely to be electrostatic interactions.

Potential alterations in the hydrogen-bonding network were evaluated in the various β-72 substituted end-point conformers. These studies indicate that NMA at β-72 restricts potential hydrogen bonding as compared to other amino acids due to the imposition of a methyl group that is incapable of hydrogen bonding. NMA-72 is located in a relatively undefined loop between helices B and E of C-PC (Duerring *et al.*, 1988). The main-chain carbonyl oxygen is located near N21 of pyrrole ring B and the amide nitrogen of Tyr-

74, and it demonstrates hydrogen bonding to each in the energy-minimized crystal structure. These two main-chain interactions are common to all β-72 substituted C-PC mutants with the exception of Asp-72, which interacts with the guanidino group of Arg-78 instead of the pyrrole ring B. While the NMA side chain yields no hydrogen-bonding interactions with local atoms, several β-72 substitutions show unique side-chain bonding patterns. In particular, the side-chain amide of Gln-72 interacts with a guanidino hydrogen of Arg-78. The amide hydrogen of Asn-72, the hydroxyl hydrogen of Ser-72, and the carboxamido oxygen of NMG interact with the hydroxyl hydrogen of Thr-122. It is likely that the addition of a methylene group to NMA, creating NMG, changes relative atom orientations that allow hydrogen bond formation. The methylene group increases NMG side-chain length by approximately 1 Å, thereby causing atom displacement. ψ and χ_1 are changed by approximately 60° and 40°, respectively, when NMA is replaced by NMG. It is clear from this evaluation of hydrogen-bonding networks that β-72 replacement has a substantial effect on the local protein structure.

The β-84 chromophore geometry was monitored for wild-type and mutant phycocyanin β subunits by calculation of a time correlation series during the production phase of dynamics. The dihedral angles of the methene bridges are less conformationally restrained than the five-membered rings of the tetrapyrrole and were monitored throughout the production phase of the dynamics trajectory. The distribution of NMA conformers is similar to that of all mutants for the angles C4−C5−C6−C7 and C8−C9−C10−C11 (data not shown). However, the methene bridge connecting rings C and D, C13−C14−C15−C16, displays a striking contrast between NMA-containing structures and all others. Figure 6 shows the fraction of total conformer population versus these selected bilin dihedral angles for the dihedral angle C13−C14−C15−C16. NMA imposes a large deviation on this methene bridge (+32°) compared to most other amino acids in which the average dihedral is approximately −40°. Perhaps the most significant evidence that NMA does alter chromophore geometry is in the comparison of this dihedral when NMA and Asn are at β-72. The *N*-methyl group obviously induces large changes in dihedral conformation. While the only difference between the two residues is a single methyl group, the conformer population for Asn is unique from that for NMA, differing by an average of 70°. Alternatively, NMG differs from NMA by the addition of a methylene group, and its dihedral angle most closely approximates that of NMA.

DISCUSSION

We and others have hypothesized that NMA "tunes" the spectroscopic properties of the β-84 chromophore, thus improving overall energy-transfer efficiency through the phycobilisome. We have demonstrated that NMA replacement affects both the ground to excited state transition and the excited state of the β-84 chromophore. This was judged by changes in the absorption maxima and steady-state fluorescence characteristics with no change in extinction coefficient. It was our goal to fortify the conclusion that β-72 substitution results in excited-state energy losses by applying time-resolved fluorescence techniques. The β-72 substitutions are expected to cause alterations in fluorescence lifetimes because both the lifetimes and the quantum yields depend on competition between radiative emission by fluorescence and processes that deactivate the excited state by nonradiative pathways. The observed effects on lifetimes when NMA is replaced clearly reflect altered photophysics of the β-84 chromophore. These kinetics results for C-PC are consistent with observed differences between control and mutant relative fluorescence quantum yields and further substantiate the hypothesis that the presence of NMA decreases nonradiative energy losses.

The spectroscopic properties of phycobiliproteins are notoriously sensitive to the aggregation state of the phycobiliprotein and the presence or absence of colorless linker polypeptides. The phycobiliprotein aggregation state is a function of pH and protein concentration as well as the linker composition. We have chosen the simplest C-PC form, the monomer, for detailed examination because this is the predominant species at pH 7.0 and the dilute protein concentrations necessary for fluorescence spectroscopy. Our gel filtration experiments establish that no higher aggregation state is detectable unless the protein concentration is conservatively more than 3-fold higher than the concentration of the fluorescence lifetime experiments. The fluorescence quantum yield data presented in Table 3 argue that the effects we observe in the isolated C-PC monomer are also expressed in the phycobilisome aggregate containing the other energy-transfer components including allophycocyanin and the colorless linker polypeptides. Our control strain contains wild-type C-PC along with the 33-kDa linker deletion so that, like the site-specific mutants, these phycobilisomes contain rods with a single disk of C-PC attached to the core (Swanson *et al.*, 1992). The observed phycobilisome quantum yields are higher than the corresponding yields in the isolated C-PC that is devoid of linkers. This is expected, as the linker polypeptides are known to interact with the β-84 chromophore in the native phycobilisome and are believed to increase bilin rigidity which effectively minimizes potential pathways of deexcitation (Glazer, 1985, 1989).

Although all three chromophores in C-PC are chemically equivalent phycocyanobilins, there are several spectroscopically distinct types that arise from their differing interactions with the surrounding apoprotein (Teale & Dale, 1970; Sauer *et al.*, 1987; Debreczeny *et al.*, 1993). Chromophore orientation is known to determine spectroscopic properties; conformational flexibility would provide a mechanism for increasing nonradiative processes. Native apophycobiliproteins act as a scaffold in constraining the chromophores to be quasilinear and, as a consequence, confer high fluorescence quantum yields and a prominent visible absorption peak to the bilin chromophores. It is this spectroscopic distinction that confers the properties of directional light energy transfer through the phycobilisome with an efficiency that exceeds 95% (Glazer, 1984). The β-84 chromophore plays an especially important role in this process, as it is the terminal acceptor of the three chromophores within C-PC disks and is responsible for interdisk transfer in the phycobilisome rods.

The photophysics of phycobiliprotein and phycobilisome fluorescence are complex, yet three lifetimes are usually discernable from experimental data (Debreczeny *et al.*, 1993; Glazer, 1985; Gillbro *et al.*, 1985; Holzwarth *et al.*, 1987; Wendler *et al.*, 1986). C-PC and the phycobilisomes contain numerous chromophores that act in concert to transfer excitation energy via the Förster energy-transfer mechanism.

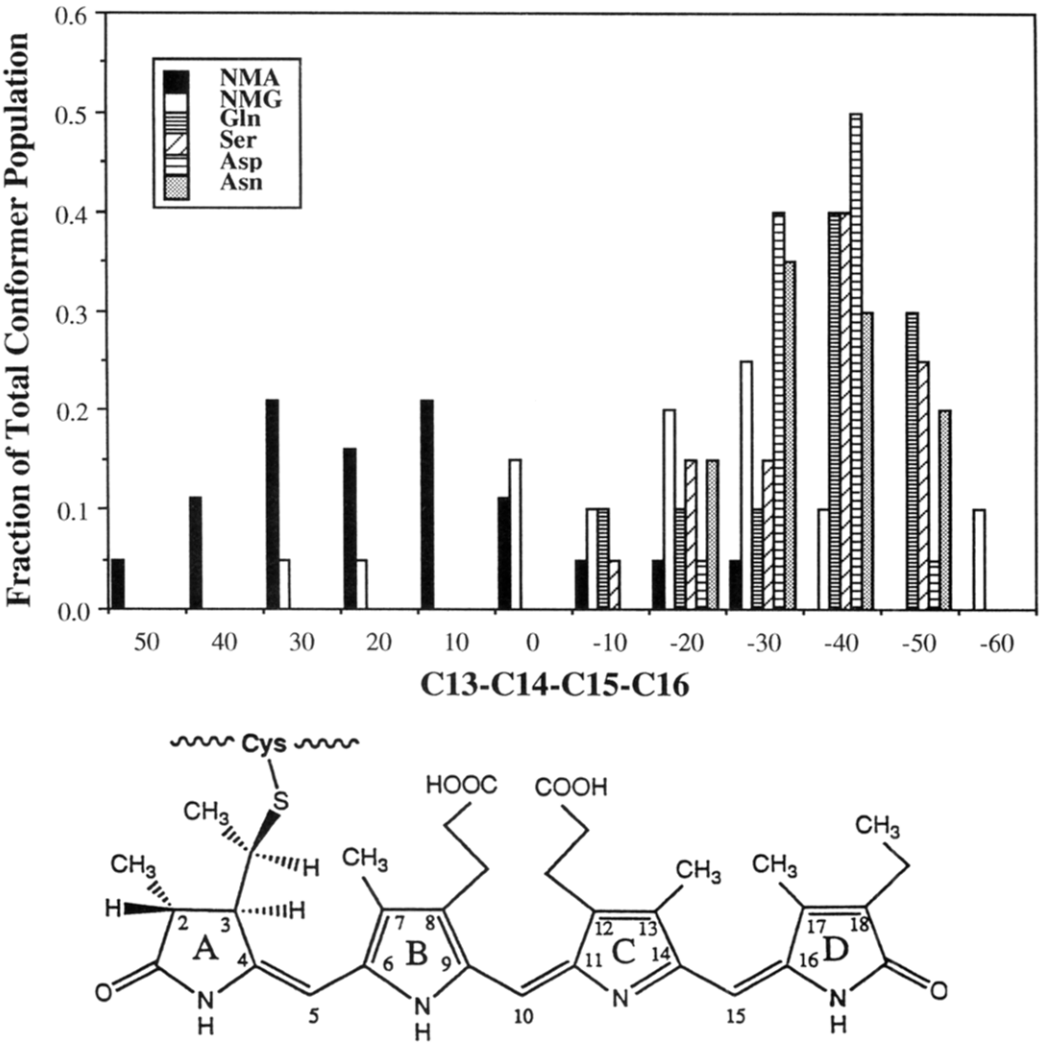

FIGURE 6: Fraction of total conformer population versus bilin chromophore dihedral angle, C14−C15−C16−C17. These data are obtained from calculation of a time series during the equilibration phase of each dynamics trajectory and represent a total of 20 conformers.

The reproducible and excellent fit to a triple-exponential decay is consistent with three spectroscopically distinguishable chromophores whose environments in phycobiliproteins are not highly variable. This is also consistent with the natural design of light-harvesting antennae which are optimized for efficient light energy transfer. High fluorescence quantum yields are conferred upon bilin chromophores by the presence of a protein scaffold which restricts conformational flexibility. This environmental restriction minimizes processes leading to nonradiative relaxation (energy losses) such as excited-state proton-transfer reactions, intersystem crossing, or photoisomerization. We consider it plausible that NMA optimizes energy transfer by altering the conformational equilibrium of the chromophore and/or restricting its flexibility.

The effects of NMA substitution in the time-resolved fluorescence experiments are interpreted in the context of previous assignments in the literature. The individual lifetimes were not assigned to discrete transfer processes because this method of interpretation requires several simplifying assumptions. Lifetime components of phycobilisomes and phycobiliproteins have previously been assigned to specific rate processes in numerous experiments by the method of selective excitation (Yamazaki *et al.*, 1984; Wendler *et al.*, 1984; Suter *et al.*, 1984; Holzwarth *et al.*, 1982) or low-temperature spectroscopy coupled with computations (Sauer *et al.*, 1987; Debreczeny *et al.*, 1993). Despite other discrepancies, the existing literature is unified by the attribution of the longest lifetime in a given light-harvesting system to the fluorescence emanating from the terminal emitters; our DAS data agree with this model.

In summary, we have shown by steady-state and time-resolved fluorescence techniques that methylation of a single asparagine has a substantial influence on the photophysics of the β-84 fluorescing chromophore by decreasing losses via nonradiative pathways of deexcitation. It was our goal to corroborate this experimental evidence with calculations using the available crystal structure coordinates of C-PC isolated from *Mastigocladus laminosus* (Schirmer *et al.*, 1987). The purpose of these molecular dynamics calculations was to evaluate the possibility that β-72 replacement affects the conformational equilibrium of the β-84 chromophore. The dynamics data indicate that NMA at β-72 yields a unique local environment in the vicinity of the β-84 chromophore which correlates with the experimental data. The most striking difference in β-84 chromophore geometry is found at the methene bridge connecting the C and D rings where *N*-methylation affords an average 70° change in

dihedral orientation relative to the other tested substitutions. It is intriguing that changes in the β-72 amino acid have such a profound effect on distant D ring chromophore dihedral angles. It is likely that the large change in ring D conformation induced by asparagine methylation is caused by numerous, compensatory variations in chromophore angles proximal to β-72 which eventually lead to a large deviation in ring D. The X-ray crystal structure indicates that ring D is poorly defined in electron density for *Agmenellum quadruplicatum* (Schirmer *et al.*, 1986). It is also less conformationally restrained in the X-ray crystal structure because it is located near the protein surface (Schirmer *et al.*, 1987). It is logical that changes in chromophore structure will first be manifested in the atoms that are most conformationally flexible.

The D ring orientation in the β-84 chromophore C-PC β subunits when NMA is replaced with alternative amino acids is highly reminiscent of the geometry for the β-155 sensitizing chromophore (Schirmer *et al.*, 1987). Our calculations imply that NMA is responsible for conferring upon the β-84 chromophore the spectral properties that make it the essential fluorescing chromophore. The data presented *vide infra* are consistent with this hypothesis, as NMA replacement yields diminished fluorescence lifetimes and quantum yields. NMA replacement also causes a blue shift in the absorbance spectrum of the isolated protein that would be consistent with the idea that the β-84 chromophore behaves more like a sensitizing chromophore under those conditions.

A limited amount of thermodynamic protein stability data has been reported for phycobiliproteins. Chen *et al.* (1977, 1994) have reported a lower apparent unfolding ΔG of 4.0−4.6 kcal/mol for *Phormidium luridum* C-PC at pH 6.0 while the urea concentration for 50% denaturation was near 4.5 M, similar to our data. However, these investigators found m values of 0.8−1.0 (m is a parameter which describes the dependence of the free energy on urea concentration), while our data reveal m values of 1.7−2.5; the reasons for these differences are not clear. Due to the problems inherent to extrapolations, we also evaluated the ΔG values of unfolding at denaturation concentrations that correspond to the midpoint of the unfolding region because this region of the transition is the most accurately determined. As a consequence of this calculation, all ΔG values for the mutants are listed as a *difference* in ΔG relative to the control and in this manner can then be compared (Pace, 1989). The $\Delta\Delta G$ values for wild type and mutants relative to the control indicate little change in stability. The observed experimental errors range from 0.2 to 0.3 kcal/mol for these experiments; therefore, the observed changes in stability are negligible. This calculation method is valid for evaluating differences among closely related proteins such as the point mutations for C-PC because this method normalizes to $m_{control}$. The observed m values are all identical (within experimental error) with the exception of that for 7002 wild type. It is intriguing that *cpc*BA/BA and 7002, which are presumably identical proteins that contain NMA at the β-72 site, demonstrate the greatest observed differences. The reasons for this are unknown but perhaps are another measure of inherent error in these measurements.

It is not surprising that introduction of a mutation at the β-72 site has little effect on protein stability when considering the β-72 position in C-PC. This site is located in a relatively undefined turn and is exposed at the surface; thus it is expected that these conditions would easily accommodate at least conservative substitutions. Swanson and Glazer (1990) have demonstrated that the thermal stability of C-PC isolated from asparagine methyltransferase mutants which contain Asn at β-72 is indistinguishable from wild type. It is possible that the observed instability of the mutant phycobilisomes is due to an effect of the substitution on higher aggregate interactions in the phycobilisome rod.

These results support an interesting structure−function relationship for asparagine posttranslational modification in proteins. This modification is not known to be present in any other proteins but is highly conserved in cyanobacteria and red algae. Our experiments yield convincing evidence that a physiologically relevant function can be attributed to this stable posttranslational methylation. Asparagine methylation is now one of the select few posttranslational methylations for which a function can be demonstrated.

ACKNOWLEDGMENT

We thank Professor Donald A. Bryant and Dr. Jianhui Zhou, Department of Molecular and Cell Biology, The Pennsylvania State University, for construction of the β-72D and β-72Q mutants; Professor Jeff Nelson, Department of Biochemistry, LSU, for building the phycocyanobilin chromophore used in the molecular modeling calculations; Professor Mary Barkley, Department of Chemistry, LSU, for access to the SLM 8000 and time-resolved fluorimeters; and Professor Lynn LaMotte, Department of Experimental Statistics, LSU, for assistance with the statistical calculations. We are also grateful for incisive comments by Professor Ken Sauer, Department of Chemistry, UC−Berkeley.

REFERENCES

Beecham, J. M., Gratton, E., Ameloot, M., Knutson, J. R., & Brand, L. (1992) in *Topics in Fluorescence Spectroscopy* (Lakowicz, J., Ed.) pp 241−301, Plenum Press, New York.

Brooks, B. R., Bruccoleri, R. E., Olafson, B. D., States, D. J., Swaminathan, S., & Karplus, M. (1983) *J. Comput. Chem. 4*, 187−217.

Bryant, D. A. (1986) *Can. Bull. Fish. Aquat. Sci. 214*, 423−500.

Bryant, D. A., Guglielmi, G., Tandeau de Marsac, N., Castets, A. M., & Cohen-Bazire, G. (1979) *Arch. Microbiol. 123*, 113−127.

Chen, C.-H., Kao, O. H. W., & Berns, D. S. (1977) *Biophys. Chem. 7*, 81−86.

Chen, C.-H., Roth, L. G., MacColl, R., & Berns, D. S. (1994) *Biophys. Chem. 50*, 313−321.

Debreczeny, M., Sauer, K., Zhou, H., & Bryant, D. A. (1993) *J. Phys. Chem. 97*, 9852−9862.

de Lorimier, R. A., Bryant, D. A., Porter, R. D., Liu, W.-Y., Jay, E., & Stevens, S. E., Jr. (1984) *Proc. Natl. Acad. Sci. U.S.A. 81*, 7946−7950.

Duerring, M., Huber, R., & Bode, W. (1988) *FEBS Lett. 236*, 167−170.

Duerring, M., Schmidt, G. B., & Huber, R. (1991) *J. Mol. Biol. 217*, 577−592.

Gardner, E. E., Stevens, S. E., & Fox, J. L. (1980) *Biochim. Biophys. Acta 624*, 187−195.

Gillbro, T., Sandström, A., Sundström, V., Wendler, J., & Holzwarth, A. R. (1985) *Biochim. Biophys. Acta 808*, 52−65.

Glazer, A. N. (1984) *Biochim. Biophys. Acta 768*, 29−51.

Glazer, A. N (1985) *Annu. Rev. Biophys. Biophys. Chem. 14*, 47−77.

Glazer, A. N. (1989) *J. Biol. Chem. 264*, 1−4.

Glazer, A. N., & Fang, S. (1973) *J. Biol. Chem. 248*, 663−671.

Glazer, A. N., & Bryant, D. A. (1975) *Arch. Microbiol. 104*, 15−22.

Glazer, A. N., Yeh, S. W., Webb, S. P., & Clark, J. H. (1985a) *Science 227*, 419−423.

Glazer, A. N., Chan, C., Williams, R. C., Yeh, S. W., & Clark, J. H. (1985b) *Science 230*, 1051−1053.
Holzwarth, A. R., Wendler, J., & Wehrmeyer, W. (1982) *Photochem. Photobiol. 36*, 479−487.
Holzwarth, A. R., Wendler, J., & Suter, G. W. (1987) *Biophys. J. 51*, 1−12.
Kawahara, K., & Tanford, C. (1966) *J. Biol. Chem. 241*, 3228−3232.
Klotz, A. V., & Glazer, A. N. (1987) *J. Biol. Chem. 262*, 17350−17355.
Klotz, A. V., Leary, J. A., & Glazer, A. N. (1986) *J. Biol. Chem. 261*, 15891−15894.
Lagarias, J. C, Klotz, A. V., Dallas, J. L., Glazer, A. N., Bishop, J. E., O'Connell, J. F., & Rapoport, H. (1988) *J. Biol. Chem. 263*, 12977−12985.
Lhoest, J., & Colson, C. (1977) *MGG, Mol. Gen. Genet. 154*, 175−180.
Lhoest, J., & Colson, C. (1981) *Eur. J. Biochem. 121*, 33−37.
Lundell, D. J., & Glazer, A. N. (1983) *J. Biol. Chem. 258*, 894−901.
McMahon, L. P., Colucci, W. J., McLaughlin, M. L., & Barkley, M. D. (1992) *J. Am. Chem. Soc. 114*, 8442−8448.
Mimuro, M., Füglistaller, P., Rümbeli, R., & Zuber, H. (1986) *Biochim. Biophys. Acta 848*, 155−166.
Pace, C. N. (1986) *Methods Enzymol. 131*, 266−280.
Pace, C. N., & Vanderburg, K. E. (1979) *Biochemistry 18*, 288−292.
Rümbeli, R., Suter, F., Wirth, M., Sidler, W., & Zuber, H. (1987) *Biol. Chem. Hoppe-Seyler 368*, 1401−1406.
Satterthwaite, F. E. (1946) *Biometrics Bull. 2*, 110−114.
Sauer, K., Scheer, H., & Sauer, P. (1987) *Photochem. Photobiol. 46*, 427−440.
Schirmer, T., Huber, R., Schneider, M., Bode, W., Miller, M., & Hackert, M. L. (1986) *J. Mol. Biol. 188*, 651−676.
Schirmer, T., Bode, W., & Huber, R. (1987) *J. Mol. Biol. 196*, 677−695.
Searle, G. F. W., Barber, J., Porter, G., & Tredwell, C. J. (1978) *Biochim. Biophys. Acta 501*, 246−256.
Stevens, S. E., Jr., Patterson, C. O. P., & Meyers, J. (1973) *J. Phycol. 9*, 427−430.
Stryjewski, W. (1991) *Rev. Sci. Instrum. 62*, 1921−1925.
Suter, G. W., Mazzola, P., Wendler, J., & Holzwarth, A. (1984) *Biochim. Biophys. Acta 766*, 269−276.
Swanson, R. V., & Glazer, A. N. (1990) *J. Mol. Biol. 214*, 787−796.
Swanson, R. V., Zhou, J., de Lorimier, R., Leary, J. A., Williams, T., Bryant, D. A., & Glazer, A. N. (1992) *J. Biol. Chem. 267*, 16146−16154.
Teale, F. W. J., & Dale, R. E. (1970) *Biochem. J. 116*, 161−169.
Thomas, B. A., Bricker, T. M., & Klotz, A. V. (1993) *Biochim. Biophys. Acta 1143*, 104−108.
Tilstra, L., Sattler, M. C., Cherry, W. C., & Barkley, M. D. (1990) *J. Am. Chem. Soc. 112*, 9176−9182.
Wendler, J., Holzwarth, A. R., & Wehrmeyer, W. (1984) *Biochim. Biophys. Acta 765*, 58−67.
Wilbanks, S. M., Wedemeyer, G., & Glazer, A. N. (1989) *J. Biol. Chem. 264*, 17860−17867.
Williams, J. G. K. (1988) *Methods Enzymol. 167*, 766−778.
Yamanaka, G., Lundell, D. J., & Glazer, A. N. (1982) *J. Biol. Chem. 257*, 4077−4086.
Yamazaki, I., Mimuro, M., Murao, T., Yamazaki, T., Yoshihara, K., & Fujita, Y. (1984) *Photochem. Photobiol. 39*, 223−240.
Zhou, J. (1992) Mutational Analysis of the Genes Encoding Phycobilisome Components in the Cyanobacterium Synechococcus PCC 7002, Ph.D. Dissertation, The Pennsylvania State University.

BI9414303